5th Asian Conference on Multibody Dynamics 2010
August 23-26, 2010, Kyoto, Japan

A UNIFIED APPROACH TO DYNAMICS OF A BIPED

S. V. Shah, S. K. Saha and J.K. Dutt

Department of Mechanical Engineering
Indian Institute of Technology Delhi
New Delhi, Delhi, 110016, India
Email: surilvshah@gmail.com, saha@mech.iitd.ac.in, jkdutt@mech.iitd.ac.in

ABSTRACT

This paper presents a unified approach for dynamic modeling and analysis of a biped. A biped is modeled as a floating-base system where the foot-ground interactions are modeled as external forces and moments. Dynamic modeling is proposed using the concept of the Decoupled Natural Orthogonal Complement (DeNOC) matrices. The equations of motion thus obtained are independent of topology of the biped. The advantage of the proposed modeling is highlighted in the paper. A numerical example of a 7-link biped is provided using the methodology presented.

1. INTRODUCTION

Research on biped is one of the active fields of robotics. There have been significant contributions in the fields of dynamics, control, and gait planning of a biped over the last two decades (Raibert, 1986; Vukobratovic et al., 1989; McGeer, 1990; Shih et al., 1993; Hirai et al., 1998; Park and Kim, 1998; Kajita et al., 2001; Collins and Ruina, 2005; Vukobratovic et al., 2007). Dynamics plays vital role in simulation and control of a biped having high joint velocities and accelerations. This paper mainly addresses an alternate method of dynamic formulation for a biped and highlights their benefits. A biped negotiates three topologies, viz., double supported, single supported and flight, during different phases of walking or running cycle. Analysis of biped dynamics may be either topology dependent or topology independent. The former approach uses different sets of equations of motion for different topologies, while the latter uses a single set of equations of motion for the complete dynamic analysis. Here, topology independent approach is used for unified modeling of a biped. This requires identifying free or floating body. Knowing the motion of the floating body, and other joint motions, dynamic analyses may be performed.

The dynamic modeling is based on the concept of Decoupled Natural Orthogonal Complement (DeNOC) matrices derived originally for a serial-chain system (Saha, 1999). The DeNOC matrices are essentially the decoupled form of the velocity transformation matrix, which when applied to Newton-Euler equations of motion, leads to a minimal set equations of motion. The DeNOC matrices were derived for a biped to obtain its dynamic model. This also helped in deriving the analytical expressions of the elements of the vectors and matrices appearing in the equations of motion, and generating recursive inverse and forward dynamics algorithms. The foot-ground interactions are taken into account as external forces and moments. This requires defining the appropriate ground model, which is represented here with the help of parallely connected spring-damper model (Voigt model) in the vertical direction and a pseudo-Coulomb friction model to avoid sliding, in the horizontal direction.

A unified dynamic formulation using the DeNOC matrices and its application for the analysis of a biped are the main contributions of this work. This paper is organized as follows: Dynamic modeling is presented in Section 2. Application of the proposed formulation is discussed in Section 3. A numerical example is provided in Section 4. Finally, conclusions are given in section 5.

2. DYNAMIC MODELING

A biped may be considered as a floating-base tree-type system as shown in Fig. 1. One of the links of the biped is assumed to be floating and denoted with number 0. Other links are numbered outward from this link, which is also referred to as the floating-base. It may be noted that numbering of a child link is higher than its parent links. Total number of links including the floating-base is given by (n+1). Next, the uncoupled Newton-Euler (NE)

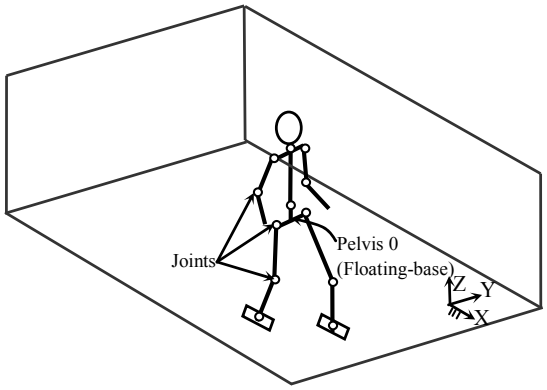

Figure 1. A BIPED

equations of motion (Chaudhary and Saha, 2009) for the rigid link *i*, denoted as #*i*, in Fig. 2, are written as

$$\mathbf{M}_i\dot{\mathbf{t}}_i + \mathbf{\Omega}_i\mathbf{M}_i\mathbf{E}_i\mathbf{t}_i = \mathbf{w}_i, \text{ where } \mathbf{w}_i \equiv \mathbf{w}_i^E + \mathbf{w}_i^C + \mathbf{w}_i^G + \mathbf{w}_i^F \tag{1a}$$

In (1a), $\mathbf{t}_i$ is the 6-dimensional vector of twist defined as $\mathbf{t}_i \equiv [\,\boldsymbol{\omega}_i^T \quad \dot{\mathbf{o}}_i^T\,]^T$, where $\boldsymbol{\omega}_i$ and $\dot{\mathbf{o}}_i$ are angular and linear velocities of link #*i* as shown in Fig. 2. Moreover, $\mathbf{\Omega}_i$, $\mathbf{M}_i$ and $\mathbf{E}_i$ are the 6×6 angular velocity, extended mass and coupling matrices for the i^{th} link. They are defined as

$$\mathbf{\Omega}_i \equiv \begin{bmatrix} \tilde{\boldsymbol{\omega}}_i & \mathbf{O} \\ \mathbf{O} & \tilde{\boldsymbol{\omega}}_i \end{bmatrix},\ \mathbf{M}_i \equiv \begin{bmatrix} \mathbf{I}_i & m_i\tilde{\mathbf{d}}_i \\ -m_i\tilde{\mathbf{d}}_i & m_i\mathbf{1} \end{bmatrix},\ \text{and } \mathbf{E}_i \equiv \begin{bmatrix} \mathbf{1} & \mathbf{O} \\ \mathbf{O} & \mathbf{O} \end{bmatrix} \tag{1b}$$

where $\tilde{\boldsymbol{\omega}}_i$ and $\tilde{\mathbf{d}}_i$ are 3×3 skew-symmetric matrices associated with vectors, $\boldsymbol{\omega}_i$ and $\mathbf{d}_i$, respectively, as shown in Fig. 2. Moreover, $\mathbf{I}_i$ and m_i are the 3×3 inertia tensor about O_i (origin of the i^{th} link), and the mass of the i^{th} link, respectively. The 6-dimensional wrench $\mathbf{w}_i$, is defined as $\mathbf{w}_i \equiv [\,\mathbf{n}_i^T \quad \mathbf{f}_i^T\,]^T$; $\mathbf{n}_i$ and $\mathbf{f}_i$ being the moment about and force at O_i for the i^{th} link, as depicted in Fig. 2. It may also be noted that in (1a) $\mathbf{w}_i^E$, $\mathbf{w}_i^C$, $\mathbf{w}_i^G$ and $\mathbf{w}_i^F$ stand for wrenches due to external moments and forces, constraints, gravity, and link-ground interaction, respectively. Next, for the (*n*+1) links, uncoupled NE equations of motion may be grouped as

$$\mathbf{M}\dot{\mathbf{t}} + \mathbf{\Omega}\mathbf{M}\mathbf{E}\mathbf{t} = \mathbf{w}^E + \mathbf{w}^C + \mathbf{w}^G + \mathbf{w}^F \tag{2}$$

where $\mathbf{\Omega}$, $\mathbf{M}$, and $\mathbf{E}$ stand for the $6(n+1)\times6(n+1)$ generalized matrices of angular velocity, extended mass, and coupling, and are given by

$$\mathbf{\Omega} \equiv \text{diag}\,[\mathbf{\Omega}_0 \quad \cdots \quad \mathbf{\Omega}_n],\ \mathbf{M} \equiv \text{diag}\,[\mathbf{M}_0 \quad \ldots \quad \mathbf{M}_n],\ \text{and}$$
$$\mathbf{E} \equiv \text{diag}\,[\mathbf{E}_0 \quad \cdots \quad \mathbf{E}_n] \tag{3}$$

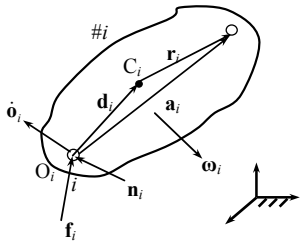

Figure 2. FREE BODY DIAGRAM OF THE i^{th} LINK

2.1 Velocity Constraints

The Decoupled Natural Orthogonal Complement (DeNOC) matrices for a tree-type biped as shown in Fig. 1 are derived in this subsection using the velocity constraints, where the velocities of each link are expressed in terms of its parent link. It is assumed that the #i^{th} link in Fig. 3, is connected to its parent link shown as #β, by an one-degree-of-freedom joint *i*, say, a revolute joint. It is pointed out here that the notation #β is introduced to signify parent body instead of #(*i*-1), as for a tree-type system the parent body need not be always #(*i*-1). The constraint equations are then written in terms of the angular and linear velocities of the origin of the links. Now, the biped is considered to have a floating-base and, hence, has n_0 degrees-of-freedom (DOF), where n_0=3 for planar, and n_0=6 for spatial motion. The constraint equations of the floating-base (#0) are then written as

$$\boldsymbol{\omega}_0 = \mathbf{L}_0\dot{\boldsymbol{\theta}}_0;\ \dot{\mathbf{o}}_0 = \mathbf{v}_0 \tag{4}$$

In (4), $\dot{\boldsymbol{\theta}}_0$, $\mathbf{L}_0$, and $\mathbf{v}_0$ are the derivative of the independent rotation co-ordinates, corresponding transformation matrix, and linear velocity vector, respectively. It may be noted that $\dot{\boldsymbol{\theta}}_0$ may contain time-rates of Euler angles or Euler-angle-joint motions (Shah et al., 2009) in the case of spatial motion or simply a scalar joint-rate for the planar motion. Next, the velocity constraints for two successive links are given as follows:

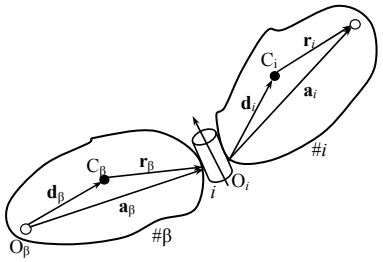

Figure 3. THE i^{th} AND ITS PARENT LINKS COUPLED BY JOINT *i*

$$\boldsymbol{\omega}_i = \boldsymbol{\omega}_\beta + \mathbf{e}_i\dot{\theta}_i\,;\;\; \dot{\mathbf{o}}_i = \dot{\mathbf{o}}_\beta + \boldsymbol{\omega}_\beta \times \mathbf{a}_{\beta,i} \tag{5}$$

In (5), $\mathbf{e}_i$ is the unit vector along the axis of rotation of the i^{th} joint and $\dot{\theta}_i$ is the corresponding joint rate. The vector $\mathbf{a}_{\beta,i}$, represents the position of O_i from O_β, which is actually $\mathbf{a}_\beta$ in Fig. 3. Next, the twist $\mathbf{t}_0$ is written from (4) as

$$\mathbf{t}_0 = \mathbf{P}_0\dot{\mathbf{q}}_0 \tag{6a}$$

where $\mathbf{P}_0$ and $\dot{\mathbf{q}}_0$ have the following representations

$$\mathbf{P}_0 \equiv \begin{bmatrix} \mathbf{L}_0 & \mathbf{O} \\ \mathbf{O} & \mathbf{1} \end{bmatrix}, \text{and } \dot{\mathbf{q}}_0 \equiv \begin{bmatrix} \dot{\boldsymbol{\theta}}_0 \\ \mathbf{v}_0 \end{bmatrix} \tag{6b}$$

In (6b) '**O**' and '**1**' stands for the null and identity matrices of compatible dimensions. Next, twist vector for the i^{th} link is written from (5) as,

$$\mathbf{t}_i = \mathbf{A}_{i,\beta}\mathbf{t}_\beta + \mathbf{p}_i\dot{\theta}_i \tag{7a}$$

In (7a), $\mathbf{A}_{i,\beta}$ is the 6×6 twist propagation matrix, and $\mathbf{p}_i$ is the 6-dimensional motion propagation vector, which are given as follows

$$\mathbf{A}_{i,\beta} \equiv \begin{bmatrix} \mathbf{1} & \mathbf{O} \\ \tilde{\mathbf{a}}_{i,\beta} & \mathbf{1} \end{bmatrix}, \text{ and } \mathbf{p}_i \equiv \begin{bmatrix} \mathbf{e}_i \\ \mathbf{0} \end{bmatrix} \text{(for a revolute pair)} \quad \text{or } \mathbf{p}_i \equiv \begin{bmatrix} \mathbf{0} \\ \mathbf{e}_i \end{bmatrix} \text{(for a prismatic pair)} \tag{7b}$$

It may be noted that in (7b) $\tilde{\mathbf{a}}_{i,\beta} = -\tilde{\mathbf{a}}_\beta$, which is the 3×3 skew-symmetric matrix associated with the vector $\mathbf{a}_\beta$. The generalized twist, and generalized independent velocities for the (n+1) coupled links are then defined as

$$\mathbf{t} \equiv \begin{bmatrix} \mathbf{t}_0^{\mathrm{T}} & \mathbf{t}_1^{\mathrm{T}} & \dots & \mathbf{t}_n^{\mathrm{T}} \end{bmatrix}^{\mathrm{T}}, \text{ and } \dot{\mathbf{q}} \equiv \begin{bmatrix} \dot{\mathbf{q}}_0^{\mathrm{T}} & \dot{\theta}_1 & \dots & \dot{\theta}_n \end{bmatrix}^{\mathrm{T}} \tag{8}$$

Substituting (6a) and (7a) into (8), the expression for the generalized twist, **t**, is obtained as

$$\mathbf{t} = \mathbf{A}\mathbf{t} + \mathbf{N}_d\dot{\mathbf{q}} \tag{9}$$

where the 6(n+1)×6(n+1) and 6(n+1)×(n+n_0), matrices **A** and $\mathbf{N}_d$ are given by

$$\mathbf{A} \equiv \begin{bmatrix} \mathbf{O} & \mathbf{O} & \cdots & \mathbf{O} \\ \mathbf{A}_{1,\beta} & \mathbf{O} & \ddots & \vdots \\ \vdots & \ddots & \ddots & \mathbf{O} \\ \mathbf{O} & \cdots & \mathbf{A}_{n,\beta} & \mathbf{O} \end{bmatrix}, \text{ and } \mathbf{N}_d \equiv \begin{bmatrix} \mathbf{P}_0 & & & \\ & \mathbf{p}_1 & & \\ & & \ddots & \\ & & & \mathbf{p}_n \end{bmatrix} \tag{10}$$

In (10), β in $\mathbf{A}_{i,\beta}$ signifies the parent of i for i = 1, …, n. Rearranging (10), the 6(n+1)-dimensional vector of generalized twist **t** is written as

$$\mathbf{t} = \mathbf{N}_l\mathbf{N}_d\dot{\mathbf{q}}, \text{ where } \mathbf{N}_l \equiv (\mathbf{1} - \mathbf{A})^{-1}. \tag{11}$$

It may be noted that '**1**' in (11) stands for the identity matrix compatible in dimension with **A**, i.e., 6(n+1)×6(n+1), whereas $\mathbf{N}_l$ and $\mathbf{N}_d$ are the desired DeNOC matrices for the tree-type biped under study. The strength of the concept of using the DeNOC matrices lies in the fact that the matrix structure remains same for all configurations of biped, be it in the flight phase or support phase. The 6(n+1)×6(n+1) lower block triangular matrix $\mathbf{N}_l$, is obtained as

$$\mathbf{N}_l \equiv \begin{bmatrix} \mathbf{1} & \mathbf{O} & \cdots & \mathbf{O} \\ \mathbf{A}_{1,0} & \mathbf{1} & \cdots & \mathbf{O} \\ \vdots & \ddots & \ddots & \vdots \\ \mathbf{A}_{n,0} & \cdots & \mathbf{A}_{n,n\text{-}1} & \mathbf{1} \end{bmatrix}, \text{ where } \mathbf{A}_{i,j} = \mathbf{O} \text{ if } i \notin \gamma_j \tag{12}$$

and γ_j is an array of all the links connected upstream from j^{th} link including j.

2.2. Equations of Motion

Pre-multiplying (2) by $\mathbf{N}_d^T\mathbf{N}_l^T$ eliminates the constraint wrenches as a result a minimal set of equations of motion is given as

$$\mathbf{N}_d^T\mathbf{N}_l^T\left(\mathbf{M}\dot{\mathbf{t}} + \boldsymbol{\Omega}\mathbf{M}\mathbf{E}\mathbf{t}\right) = \mathbf{N}_d^T\mathbf{N}_l^T(\mathbf{w}^E + \mathbf{w}^G + \mathbf{w}^F) \tag{13}$$

where $\mathbf{N}_d^T\mathbf{N}_l^T\,\mathbf{w}^C$ vanishes (Angeles and Ma, 1988). Substituting (11) and its time derivatives into (13), and rearranging the terms, one obtains the following:

$$\mathbf{I}\ddot{\mathbf{q}} + \mathbf{C}\dot{\mathbf{q}} = \boldsymbol{\tau} + \boldsymbol{\tau}^G + \boldsymbol{\tau}^F \tag{14}$$

where the expressions for the generalized inertia matrix (GIM) **I**, matrix of convective inertia (MCI) **C**, and vectors of the generalized external force $\boldsymbol{\tau}$, generalized force due to

gravity $\boldsymbol{\tau}^G$, and the forces due to foot-ground interaction $\boldsymbol{\tau}^F$ are given as

$$\begin{aligned}&\mathbf{I} \equiv \mathbf{N}^T\mathbf{M}\mathbf{N},\ \mathbf{C} \equiv \mathbf{N}^T(\mathbf{M}\dot{\mathbf{N}} + \boldsymbol{\Omega}\mathbf{M}\mathbf{E}\mathbf{N}), \boldsymbol{\tau} \equiv \mathbf{N}^T\mathbf{w}^E,\\ &\boldsymbol{\tau}^G \equiv \mathbf{N}^T\mathbf{w}^G \text{ and } \boldsymbol{\tau}^F \equiv \mathbf{N}^T\mathbf{w}^F;\ \mathbf{N} \equiv \mathbf{N}_l\mathbf{N}_d\end{aligned} \tag{15}$$

It may be noted that the vector $\mathbf{w}^F$ is obtained from a suitable foot-ground interaction model. It is modeled here as a spring-damper system in the vertical direction and pseudo-coulomb friction in horizontal direction to avoid sliding (Shah et al., 2006).

3. APPLICATION

The dynamic formulation presented in the previous section using the DeNOC matrices helps in obtaining the analytical expression of vector and matrices which appear in the equations of motion. This in turn facilitates the uniform development of recursive inverse and forward dynamics. In this section analytical expressions for the elements of the generalized inertia matrix are obtained and the steps leading to recursive inverse and forward dynamics algorithms are outlined.

3.1. Analytical Expression of the Generalized Inertia Matrix

The generalized inertia matrix of (15) can also be written as

$$\mathbf{I} = \mathbf{N}_d^T\tilde{\mathbf{M}}\mathbf{N}_d, \text{ where } \tilde{\mathbf{M}} = \mathbf{N}_l^T\mathbf{M}\mathbf{N}_l \tag{16}$$

In (16), the matrix $\tilde{\mathbf{M}}$ is referred to as the generalized composite mass matrix. Substituting $\mathbf{N}_l$ and $\mathbf{M}$ from (12) and (3) into (16), the analytical expressions for the block elements of $\tilde{\mathbf{M}}$ are obtained as follows:

For $i = 0, \ldots, n$, and $j = 0, \ldots, i$

$$\begin{aligned}&\tilde{\mathbf{M}}_{i,j} = \tilde{\mathbf{M}}_i\mathbf{A}_{i,j}, \text{ if } i \in \gamma_j, \text{ and } \tilde{\mathbf{M}}_{j,i} = \tilde{\mathbf{M}}_{i,j},\\ &\mathbf{A}_{i,j} = \mathbf{1} \text{ when } i = j \text{ and} = \mathbf{O} \text{ if } i \notin \gamma_j\end{aligned} \tag{17}$$

In (17) $\mathbf{A}_{i,j}$ is the 6×6 twist propagation matrix defined similar to $\mathbf{A}_{i,\beta}$ of (7b). Moreover $\tilde{\mathbf{M}}_i$ is the 6×6 matrix of the composite body i which comprises of all rigidly attached links upstream from the i^{th} link. It is obtained recursively as follows:

$$\tilde{\mathbf{M}}_i = \mathbf{M}_i + \sum_{\xi_i \in j} \mathbf{A}_{j,i}^T\tilde{\mathbf{M}}_j\mathbf{A}_{j,i} \tag{18}$$

where ξ_i denotes children of the i^{th} link. The analytical expression for each term of the generalized inertia matrix $\mathbf{I}$ of (16) can then be obtained as follows:

For $i = 0, \ldots, n$, and $j = 0, \ldots, i$

$$\begin{aligned}&I_{i,j} = \mathbf{p}_i^T\tilde{\mathbf{M}}_{i,j}\mathbf{p}_j, \text{ if } i, j \geq 1,\\ &\text{and } \mathbf{p}_i = \mathbf{P}_0, \text{ if } i = 0, \text{and } \mathbf{p}_j = \mathbf{P}_0, \text{ if } j = 0\end{aligned} \tag{19}$$

The analytical expression in (19) serves as the foundation for obtaining a recursive inverse or forward dynamics algorithm for the tree-type system at hand. Decoupling the motion of floating-base from the rest of the system, the equations of the motion in (14) are expressed as

$$\begin{bmatrix}\mathbf{I}_0 & \tilde{\mathbf{I}}^T\\ \tilde{\mathbf{I}} & \bar{\mathbf{I}}\end{bmatrix}\begin{bmatrix}\ddot{\mathbf{q}}_0\\ \ddot{\boldsymbol{\theta}}\end{bmatrix} = \begin{bmatrix}\mathbf{0}\\ \bar{\boldsymbol{\tau}}\end{bmatrix} + \boldsymbol{\varphi} \tag{20}$$

where $\mathbf{I}_0$ is the $n_0 \times n_0$ matrix associated with floating base, $\bar{\mathbf{I}}$ is the $n \times n$ matrix associated with the rest of the tree-type biped, $\tilde{\mathbf{I}} \equiv \begin{bmatrix}\mathbf{I}_{1,0}^T & \ldots & \mathbf{I}_{n,0}^T\end{bmatrix}^T$, $\bar{\boldsymbol{\tau}} \equiv \begin{bmatrix}\boldsymbol{\tau}_1^T & \ldots & \boldsymbol{\tau}_n^T\end{bmatrix}^T$, and $\boldsymbol{\varphi} \equiv \boldsymbol{\tau}^G + \boldsymbol{\tau}^F - \mathbf{C}\dot{\boldsymbol{\theta}}$.

3.2 Inverse Dynamics

Inverse dynamics involves the computation of accelerations of the floating-base followed by the joint torques. It helps in model-based feedforward control of the legged robots. Inverse Dynamics problem is formulated here using (20) as

$$\begin{aligned}&\ddot{\mathbf{q}}_0 = \mathbf{I}_0^{-1}\tilde{\boldsymbol{\varphi}}_\mathbf{0}, \text{ where } \tilde{\boldsymbol{\varphi}}_\mathbf{0} \equiv (\boldsymbol{\varphi}_\mathbf{0} - \tilde{\mathbf{I}}^T\ddot{\boldsymbol{\theta}})\\ &\bar{\boldsymbol{\tau}} = \tilde{\mathbf{I}}\ddot{\mathbf{q}}_0 - \tilde{\boldsymbol{\varphi}}, \text{where } \tilde{\boldsymbol{\varphi}} \equiv (\boldsymbol{\varphi} - \mathbf{I}\ddot{\boldsymbol{\theta}})\end{aligned} \tag{21}$$

Equations in (21) are solved recursively with the help of the DeNOC matrices. Detailed steps of the recursive dynamics algorithm are not shown here, however, the basic philosophy is stated below:

Step 1: Find $\mathbf{t}$, $\mathbf{t}'$, and $\mathbf{w}^* = \mathbf{w}^F - (\mathbf{M}\mathbf{t}' + \boldsymbol{\Omega}\mathbf{M}\mathbf{E}\mathbf{t})$

In this step $\mathbf{t}_i$, $\mathbf{t}_i'$, and $\mathbf{w}_i^*$ (for $i = 0, \ldots, n$) are obtained recursively for each link starting from the floating-base. It may be noted that $\mathbf{t}'$ is the generalized twist-rate vector while $\ddot{\mathbf{q}}_0 = \mathbf{0}$.

Step 2: Find $\tilde{\boldsymbol{\varphi}} = \mathbf{N}_d^T\mathbf{N}_l^T\mathbf{w}^*$, and $\mathbf{I}_0$, $\tilde{\mathbf{I}}$

Having the results of Step 1, this step computes $\tilde{\boldsymbol{\varphi}}_i$, $\tilde{\mathbf{M}}_i$, $\mathbf{I}_0$, and $\mathbf{I}_{i,0}$ (for $i = n, \ldots, 0$) using backward recursions.

Step 3: Find $\ddot{\mathbf{q}}_0 = \mathbf{I}_0^{-1}\tilde{\boldsymbol{\varphi}}_\mathbf{0}$, and $\boldsymbol{\tau} = \tilde{\mathbf{I}}\ddot{\mathbf{q}}_0 - \tilde{\boldsymbol{\varphi}}$

Finally, accelerations of the floating-base $\ddot{\mathbf{q}}_0$, and the joint torques, τ_i (for $i = 1, \ldots, n$) are obtained.

3.2 Forward Dynamics

Forward dynamics problem attempts to find the joint motions from the knowledge of the external joint torques and forces. This enables simulation studies where the configuration of the system at hand is obtained. Forward dynamics problem is written as

$$\ddot{\mathbf{q}} = \mathbf{I}^{-1}\boldsymbol{\varphi}', \text{ where } \boldsymbol{\varphi}' = \boldsymbol{\tau} + \boldsymbol{\varphi} \tag{22}$$

The recursive forward dynamics algorithm developed here is based on the reverse Gaussian elimination and the $\mathbf{UDU}^T$ decomposition of the generalized inertia matrix $\mathbf{I}$ of (14). Here, only outline of the recursive forward dynamics algorithm is presented.

Step 1: Computation of $\boldsymbol{\varphi}'$

It requires similar steps as computation of $\tilde{\boldsymbol{\varphi}}$ in inverse dynamics algorithm.

Step 2: $\mathbf{UDU}^T$ decomposition of the GIM

In this step, the generalized inertia matrix is factorized as $\mathbf{I}=\mathbf{UDU}^T$, where $\mathbf{U}$ and $\mathbf{D}$ are an upper triangular and a diagonal matrix, respectively. The analytical expressions of the elements of $\mathbf{U}$ and $\mathbf{D}$, i.e., $U_{i,j}$ and D_i, are obtained, e.g., in (Saha, 1997) for serial system, that establish the recursive relationships.

Step 3: Solution of joint accelerations, $\ddot{\mathbf{q}} = \mathbf{U}^{-T}\mathbf{D}^{-1}\mathbf{U}^{-1}\boldsymbol{\varphi}'$

The joint accelerations are solved recursively using three sets of linear algebraic equations, namely

i) $\mathbf{U}\hat{\boldsymbol{\varphi}}' = \boldsymbol{\varphi}'$, where $\hat{\boldsymbol{\varphi}}' = \mathbf{D}\mathbf{U}^T\ddot{\boldsymbol{\theta}}$

ii) $\mathbf{D}\tilde{\boldsymbol{\varphi}}' = \hat{\boldsymbol{\varphi}}'$, where $\tilde{\boldsymbol{\varphi}}' = \mathbf{U}^T\ddot{\boldsymbol{\theta}}$

iii) $\mathbf{U}^T\ddot{\boldsymbol{\theta}} = \tilde{\boldsymbol{\varphi}}'$

4. A NUMERICAL EXAMPLE

A numerical example is given with respect to a 7-link biped as shown in Fig. 4. The recursive inverse and forward dynamics results are reported. For that the center of mass (COM) (X_0, Y_0, Z_0) and the Euler angles (φ_0, θ_0, ψ_0) are assumed to be the generalized independent coordinates for the floating-base #0, i.e., the trunk. It is assumed that the biped moves in a sagittal plane and hence X_0, Y_0, and φ_0 are the only generalized coordinates for the floating-base as others are constant. Moreover θ_1 to θ_6 are also the independent generalized coordinates for the 9-DOF biped, as shown in Fig. 4. The length and mass of the links are

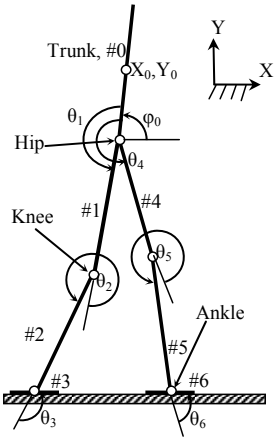

Figure 4. A 7-LINK BIPED

taken as l_0= 0.5m, l_1= l_2= l_4= l_5= 0.5 m, l_3= l_6= 0.15m, m_0 = 5 Kg, and m_1= m_2 = m_4 = m_5 = 1 Kg, and m_3= m_6 = 0.2 Kg.

Inverse dynamics problem involves the calculation of the accelerations of trunk followed by the computation of joint torques. For this, the trajectories of foot and the COM of the trunk are synthesized first. It is assumed that mass of the biped is concentrated at hip and the feet remain horizontal throughout its motion cycle. It is also assumed that trunk remains vertical throughout the walking cycle, i.e., φ_0=90^o and its height remains constant, i.e., Y_0=y_c. Hence, COM of trunk has similar motion as that of the hip. Hip trajectories are designed using the inverted pendulum mode (Park and Kim, 1998; Kajita et al., 2001). Hip trajectories for one cycle with time period of T are taken as follows:

For $0 \le t \le T$

$$\begin{aligned} x_{hip}(t) &= x_i \cosh(wt) + \left(\frac{\dot{x}_i}{w}\right)\sinh(wt) \\ y_{hip}(t) &= y_c - \left(\frac{l_0}{2}\right) \end{aligned} \tag{23}$$

where x_i and $\dot{x}_i$ are the initial position and velocity, and $w = \sqrt{g/y_c}$. The repeatability conditions $x_0 = -x_T$ and $\dot{x}_0 = \dot{x}_T$ are used to obtain x_{hip} trajectory. Ankle trajectories are then synthesized as a cosine function, i.e.,

$$\begin{aligned} x_{ankle}(t) &= -l_s \cos\left(\frac{\pi}{T}t\right) \\ y_{ankle}(t) &= \frac{h_f}{2}\left[1 - \cos\left(\frac{\pi}{T}t\right)\right] \end{aligned} \tag{24}$$

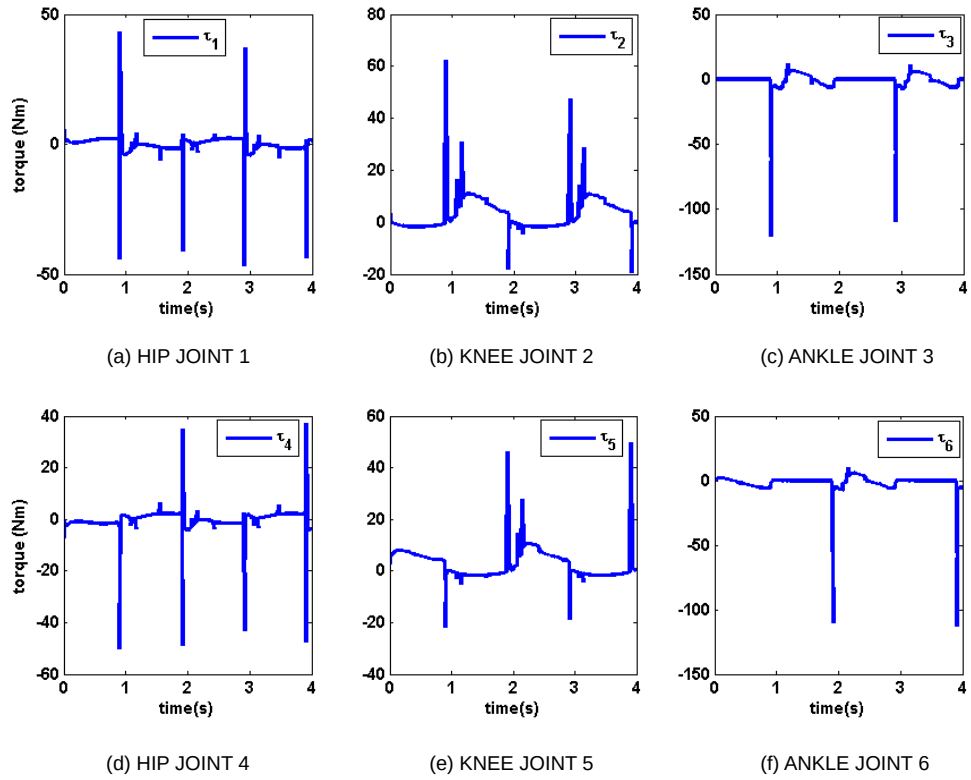

(a) HIP JOINT 1 (b) KNEE JOINT 2 (c) ANKLE JOINT 3

(d) HIP JOINT 4 (e) KNEE JOINT 5 (f) ANKLE JOINT 6

Figure 5. JOINT TORQUES

In (24), l_s, and h_f are stride length, and maximum foot height respectively. The values of T, l_s, h_f, and y_c are taken as 1sec, 0.2m, 0.1m, and 1.23m, respectively. The trajectories at the joint levels, i.e., θ_1 to θ_6 are calculated using inverse kinematics relations for the biped. Those trajectories were used to obtain the trunk motions, followed by the evaluation of joint torques. Figure 5 shows torques required at different joints. The sudden variations in the joint torques at the end of each cycle are mainly due to the compliant nature of the foot-ground interaction model. Moreover, the joint torques at ankles, i.e., τ_3 and τ_6, are zero when the foot is on the ground, which is as expected.

Next the forward dynamics was studied to simulate the controlled motion of a biped. It is done using model-based nonlinear feedforward control, where the joint torques obtained from an inverse dynamics algorithm are fed forward to the controller. The feedforward control law (Craig, 2006) may be written as

$$\boldsymbol{\tau} = \begin{bmatrix} \mathbf{0} \\ \overline{\boldsymbol{\tau}} \end{bmatrix} = \begin{bmatrix} \mathbf{0} \\ \overline{\boldsymbol{\tau}}_{ID} + \mathbf{K}_p(\boldsymbol{\theta}_d - \boldsymbol{\theta}) + \mathbf{K}_v(\dot{\boldsymbol{\theta}}_d - \dot{\boldsymbol{\theta}}) \end{bmatrix} \qquad (25)$$

where

$\mathbf{K}_p = diag\begin{bmatrix} k_{p_1} & \cdots & k_{p_n} \end{bmatrix}$, $\mathbf{K}_d = diag\begin{bmatrix} k_{d_1} & \cdots & k_{d_n} \end{bmatrix}$, and

k_{p_i} and k_{d_i} are taken as 170 and 30, respectively.

Controlled simulation was performed using the recursive forward dynamics algorithm for the time period of 4 seconds. Figures 6 and 7 show the variation in the COM and Euler angles for the trunk. It is evident from Fig. 6 that biped moves in the forward direction (i.e., X) with stable periodic motion. The slight variation in φ_0 as depicted in Fig. 7 is due to the assumption that biped mass is concentrated at hip. The joint coordinates associated with the legs, i.e., θ_1 to θ_6 are also shown in Figs. 8 and 9, which also show a periodic behavior.

In order to validate the above results the principle of energy conservation is used. The total energy is the sum of the kinetic energy (KE), potential energy (PE), ground energy and actuator energy. Figure 10 shows the variation of energies for the time period of 4 seconds. It may be seen that the total energy remains constant throughout the simulation period. All the above results are obtained using a program developed in MATLAB (2007) environment.

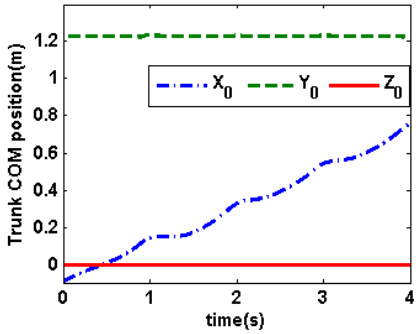

Figure 6. COM COORDINATES FOR TORSO

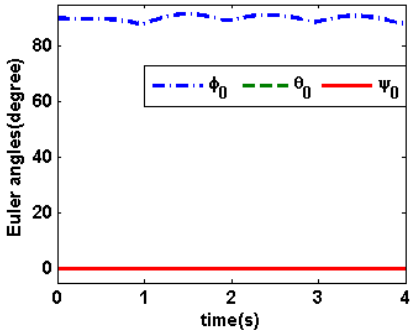

Figure 7. EULER ANGLES FOR TRUNK

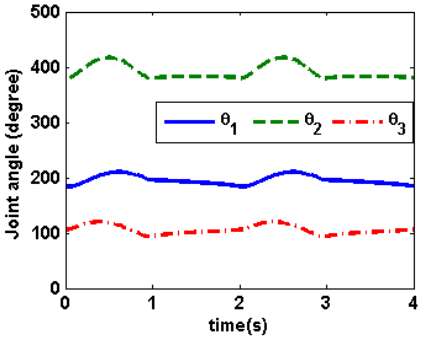

Figure 8. JOINT ANGLES FOR LEG 1

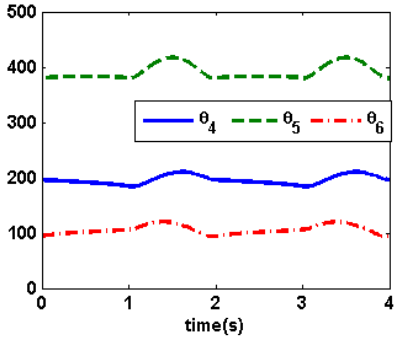

Figure 9. JOINT ANGLES FOR LEG 2

Moreover, the methodology presented is applicable to other legged robots without any change in the formulation.

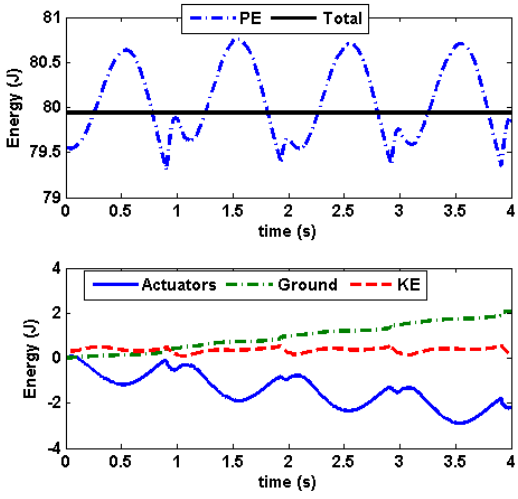

Figure 10. VARIATION OF ENERGIES

5. Conclusions

This paper presents a unified approach for the topology independent dynamic modeling of a biped. The Decoupled Natural Orthogonal Complement (DeNOC) matrices were used to obtain the dynamic model of a biped. It helped in obtaining recursive inverse and forward dynamics algorithms. A numerical example with a 7-link 9-DOF biped is presented in support of the formulations. The results have been validated using the principle of energy conservation. The proposed approach is readily applicable for dynamic analysis of the other legged robots as well.

REFERENCES

Angeles, J., and Ma, O., Dynamic simulation of n-axis serial robotic manipulators using a natural orthogonal complement. *Int. J. of Robotics Research*, Vol. 7, No. 5, pp. 32–47, 1988

Chaudhary, H., and Saha, S. K. *Dynamics and Balancing of Multibody Systems*, Springer, Berlin, 2009.

Collins, S. H., and Ruina, A. A Bipedal Walking Robot with Efficient and Human-Like Gait, *IEEE Int. Conf. on Robotics and Automation*, pp. 1983-1988, 2005.

Craig, J., J., *Introduction to Robotics Mechanics and Control*. Pearson Education, Delhi, 2006

Hirai, K., Hirose, M., Haikawa, Y., and Takenaka, T. The Development of Honda Humanoid Robot. *IEEE Int. Conf. on Robotic and Automation*, pp. 1321 – 1326, 1998.

Kajita,S., Kanehiro,F., Kaneko,K., Yokoi, K., and Hirukawa, H., The 3D Linear Inverted Pendulum Mode: A simple modeling for a biped walking pattern generation, *Int. Conf. on Intelligent Robots and Systems*, pp.239-246, 2001.

Matlab, Version 7.4 Release 2007a, MathWorks, Inc., 2007.

McGeer, T, Passive Dynamic Walking, *Int. J. Robotics Research*, Vol. 9, No. 2, pp. 62-82, 1990.

Park J. H. and Kim, K. D., Biped Robot Walking Using Gravity-Compensated Inverted Pendulum Mode and Computed Torque Control, *IEEE Int. Conf. Robotics and Automation*, pp. 3528-3533, 1998

Raibert, M. H. *Legged Robot That Balance*. MIT press, Cambridge, Massachusetts, 1986.

Saha S. K., A Decomposition of the Manipulator Inertia Matrix, *IEEE Trans. on Robotics and Automation*, Vol. 13, No. 2, pp. 301-304, 1997.

Saha, S. K. Dynamics of Serial Multibody Systems Using the Decoupled Natural Orthogonal Complement Matrices, *ASME J. of Applied Mechanics*, Vol. 66, pp. 986-996, 1999.

Shah, S. V., Mistri, B. D., and Issac, K. K., Evaluation Of Foot Ground Interaction Model Using Monopod Forward Hopping, *PCEA-IFTOMM Int. Con. on Recent Trends in Automation & its Adaptation to Industries*, 2006.

Shah, S. V., Saha, S. K., and Dutt, J. K., Denavit-Hartenberg Parameters of Euler-angle-joints for order (*n*) recursive forward dynamics, *ASME Int. conf. on Multibody systems, Nonlinear Dynamics and control*, 2009.

Shih, C. L., Gruver, W. A., and Lee, T. T., Inverse kinematics and inverse dynamics for control of a biped walking machine, *J. of Robotic Systems*, Vol. 10, No. 4, pp. 531-555, 1993.

Vukobratovic, M., Borovac, B., Surla, D. and Stokic, D., *Biped Locomotion: Dynamics, Stability, Control and Application*. Springer, Berlin, 1989.

Vukobratovic, M., Potkonjak, V., Babkovic, K., Borovac, B., Simulation model of general human and humanoid motion, *Multibody System Dynamics*, Vol. 17, No. 1, pp. 71-96, 2007.